

Nanoscaling of Microdomain Spacings in Thin Films of Cylinder-Forming Block Copolymers

Armin Knoll,[†] Larisa Tsarkova,* and Georg Krausch

Physikalische Chemie II, Universität Bayreuth, 95440 Bayreuth, Germany

Received January 2, 2007; Revised Manuscript Received January 26, 2007

ABSTRACT

We present first quantitative measurements of the characteristic lateral dimensions in thin films of cylinder-forming block copolymers. Using a metrological scanning force microscope and tailor-made image analysis, we map out lateral distances with subnanometer accuracy. Microdomain spacings change in a systematic way as a function of the film thickness and as a function the lateral cylinder bending. We show that in very thin films the unit cell is stretched perpendicular to the plane of the film resulting in lateral distances smaller than those in bulk. The changes are distinct, although small, and can be rationalized within the framework of the strong segregation theory of block copolymers.

The spontaneous formation of ordered nanostructures via self-assembly of block copolymers has recently attracted increasing interest both scientifically and in view of a growing number of technological applications.^{1,2} Block copolymers are long chain molecules consisting of two or more blocks of different chemical nature. The two blocks tend to phase separate, however, due to their connectivity on a molecular scale, phase separation on macroscopic scales is impossible. This frustration leads to the formation of highly regular domain structures with molecular dimensions, so-called microdomains. The characteristic spacing of such microdomains can be precisely controlled in the range of 10–100 nm by changing the molecular weight of the block copolymer.^{3,4} In the bulk of block copolymers, the measurements of microdomain spacings have typically been done by small-angle X-ray scattering (SAXS) and the results are widely in line with the theoretical predictions.⁵

Earlier theoretical and experimental studies on block copolymer thin films have explored the effects of the finite film thickness and the preference of the boundary surfaces to one or the other block on the resulting morphologies.^{4,6} The response of the characteristic microdomain dimensions on the confinement between two solid surfaces has been measured on multilayered lamella systems using neutron reflectivity.^{7–9} The lamella period was shown to deviate from that in bulk in a cyclic manner as a function of the confined film thickness.⁸ However, by removal of one of the confining walls, this frustration is relieved⁹ as the free film surface is able to self-adjust to the thickness constraint by the formation of islands and holes with the equilibrium thickness.⁶

Despite the considerably higher technological potential of thin films of non-lamella-forming block copolymers, up to now no quantitative experiments on characteristic lengths have been reported. This is most likely due to the experimental difficulty to accurately measure lengths when scattering experiments are not applicable. The experimental error involved in conventional scanning force microscopy (SFM) length measurements amounts to some 10–15% due to nonlinearities of the piezoelectric elements. Moreover, the lateral structures in thin block copolymer films are often characterized by a high defect density rendering an accurate measurement of the microdomain spacings difficult.

In this Letter we describe first experiments aiming at quantifying the characteristic lateral spacings in thin films of cylinder forming diblock and triblock copolymers. We use an SFM optimized for metrological measurements. The experimental results are compared with calculations based on the strong segregation theory (SST) for block copolymers.

The materials under study are composed from polystyrene (PS) and polybutadiene (PB) blocks. A diblock copolymer (SB) and a triblock copolymer (SBS) have weight averaged molecular weights of $M_w = 47.3$ kg/mol and $M_w = 102$ kg/mol, respectively, and a PS volume fraction of $f_{PS} = 26\%$. In bulk both materials form a hexagonal array of PS cylinders embedded in a PB matrix.^{10,11} The equilibration of thin films by vacuum annealing and by solvent annealing have recently been described together with the resulting phase behavior.^{10–13} For the solvent annealing, we exposed spin-coated films to a controlled atmosphere of chloroform (CHCl_3), a common solvent for both components. SFM topography and phase images were recorded in TappingMode using a Dimension 3100M microscope (Veeco Instruments) at room temperature. The microscope is based on piezo elements operated in active

* Corresponding author: larisa.tsarkova@uni-bayreuth.de.

[†] Present address: IBM Research GmbH, Säumerstrasse 4, CH-8800 Rüschlikon, Switzerland.

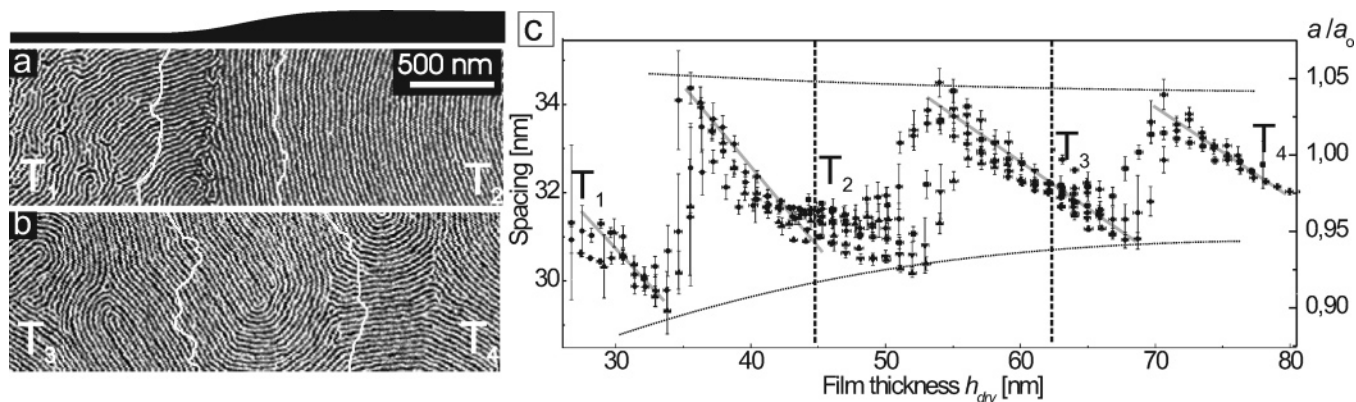


Figure 1. (a, b) SFM phase images of quenched SB films that have been annealed in CHCl_3 vapor at a polymer volume fraction ϕ of 0.7. PS cylinders appear as white stripes in a dark PB matrix. The white contour lines mark the borders of the terraces with the favored film thickness. (c) Absolute microdomain spacings (LHA) and reduced spacings (RHA) vs the thickness h_{dry} of quenched films. Different symbols correspond to different measurements and experiments. The vertical dashed lines indicate the energetically favored film thicknesses at terraces T_n . The straight gray lines emphasize different slopes of spacing relaxation upon accommodation of the next layer of cylinders. Two dotted lines follow the minimum and maximum deviations of the macrodomain spacings from a_0 , where a_0 is the spacing in the bulk.

feedback mode in all three dimensions; as a consequence, length measurements are possible with an experimental error smaller than 1 nm. The SFM images are evaluated using a tailor-made image analysis procedure to reliably determine the lateral spacing even in presence of a large number of structural defects. Details of the procedure are described in the Supporting Information.¹⁴

Upon being annealed, spin-coated films adopt macroscopically large flat regions with preferred film thickness corresponding to an integer number of layers (with a period close to the bulk interlayer spacing c_0). We refer to such terraces as T_1 , T_2 , ..., T_n indicating one, two, and n layers of cylinders, respectively. Parts a and b of Figure 1 show characteristic SFM phase images of neighboring terraces in SB films after annealing in solvent vapor. The structures are characterized by striped patterns indicative of PS cylinders embedded in a PB matrix. The white contour lines are taken from the corresponding height images (not shown here). They mark the borders between two relatively flat terraces (local energetic minimum) and an area with increasing film thickness in between. In Figure 1c the characteristic distance between the cylinders is plotted as a function of the local thickness of the film after the quench. The latter is extracted from the corresponding SFM height images. Figure 1c combines data taken from different samples and from different measurements (different symbols), each presenting two neighboring terraces and the transition region in between. Quite strikingly, we observe a systematic variation of the lateral spacing between the cylinders as the film thickness increases from n to $n + 1$ layers of cylinders. On increase of the local film thickness above n layers, the lateral distances first decrease indicating the stretching of a unit cell perpendicular to the plane of the film. Then the spacing increases rather abruptly when the excess of the stretching energy exceeds the energy needed to accommodate an additional layer of cylinders. This inclusion comes along with an overall compression of the unit cell and consequently with an increase of the lateral spacing. If the film thickness is further increased, the lateral spacing can relax to its preferred value.

Similar scaling of cylinder spacings with the film thickness was observed in SBS films (not shown here).¹³ The degree of stretching clearly decreases with increasing number of layers of cylinders as the deformation is distributed between a larger number of unit cells (dotted lines in Figure 1c). Note that the overall variation of the lateral distance amounts to only some 10% of the characteristic spacing, which would be hidden by the experimental error if either a conventional SFM would be used or distances at defects would be allowed to enter the data.

We note that the zigzag variation of the microdomain spacing on inclusion of an additional layer of cylinders qualitatively resembles the findings of Lambooy et al.⁸ on confined multilayered lamellar systems. However, in contrast to the situation studied by Lambooy et al., here the film thickness is not imposed on the system by external constraints but adjusts itself spontaneously in the region between adjacent terraces. Additionally, our films are thinner (one to five layers), and therefore the free energy difference between the contracted and expanded multilayers is more pronounced. Moreover, the situation in cylinder-forming systems appears considerably more complex than that in lamellar thin films. Earlier it has been shown that in swollen SBS films the cylinders orient perpendicular to the film plane at the transition from n to $n + 1$ layers.¹² In additional experiments, SB films were floated off the mica substrate, flipped around, and investigated from the bottom. These experiments indicate that the transition from T_1 to T_2 layers proceeds via the formation of hybrid structures such as cylinders with necks facing the bottom of the film.¹⁷ We note that the experimentally measured topography of the step region together with the direct visualization and digital analysis of the microdomain structures could be quantitatively analyzed in terms of competition between interfacial tension of the free surface and stretching of the microdomain repeat distance. This problem is however beyond the scope of the present study.

Further we find that the lateral cylinder spacing a_i within the individual terrace deviates from the respective bulk value a_0 and increases with increasing terrace number i . Figure 2a

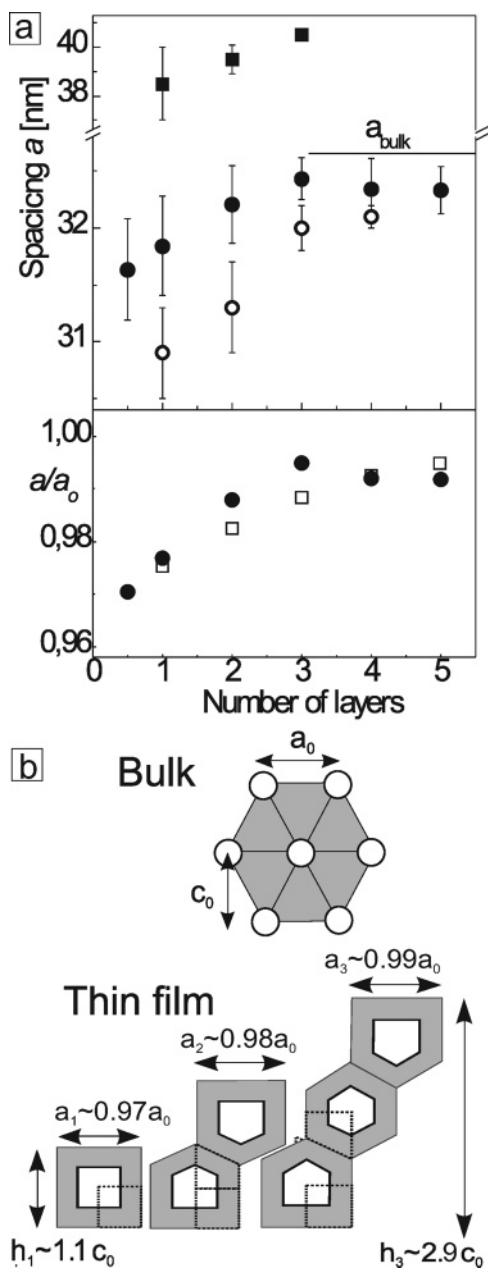


Figure 2. (a) (upper plot) Absolute spacings of cylindrical surface structures vs the number of layers measured in SB films annealed at 493 K (filled circles) in swollen SB films (open circles) and swollen SBS films (squares) with polymer volume fractions ϕ of 0.70 and 0.62, respectively. The horizontal axis corresponds to an integer number of cylinder layers and does not account for the existing wetting layer on the substrate.^{10,11} (lower plot) Comparison of the reduced microdomain dimensions measured in thermally annealed SB films (circles) with the results of the SST calculations (squares). (b) Schematics of a regular hexagonal pattern in the bulk and of the unit cells in thin films used for the SST calculation. The dotted lines denote the actual calculated geometries. The indicated a_i and h_i parameters are the results of the SST calculation.

summarizes this effect for different block copolymers and different equilibration procedures. The data indicate that the average spacing between neighboring cylinders at the energetically favored thickness is the smallest in the first terrace and eventually approaches the bulk value for films consisting of three and more layers of cylinders. The overall effect amounts to some 3% of the characteristic spacing in

thermally annealed films (Figure 2a, lower plot) and to some 6% in solvent swollen SB and SBS films (not shown). The large error bars in Figure 2a arise from the averaging over a large number of different measurements performed on different samples. (The error of an individual measurement is considerably smaller; see, e.g., Figure 1c.) However, the effect itself is clearly measurable. The fact that different block copolymer architectures and different annealing procedures lead to the same observation suggests that the effect is of general nature.

To rationalize the above finding, we employ a version of the SST for block copolymers introduced by Olmsted and Milner.^{15,16} Within this model the free energy of rather complex block copolymer microdomain structures can be calculated by subdividing the respective unit cells into infinitesimal wedges. The wedges locally enforce the conservation of the polymer volume fraction. Here only straight wedges are considered, i.e., straight paths of the molecules through the AB domain boundary. The unit cells suitable to describe the microdomain structure in thin films of cylinder forming block copolymers are shown in Figure 2b. A single layer of cylinders is described by a rectangular unit cell while a n -layers thick film will consist of $(n - 2)$ layers of hexagonal unit cells bounded by suitably modified top and bottom unit cells. For calculations, it is sufficient to consider only the parts of the unit cells which are indicated by the dotted lines. Note that due to the straight wedge constraint, the cores of the unit cells have the same shape as the unit cell itself.

In order to account for thickness variations of the polymer film, we consider a stretching factor b which quantifies the deformation of the unit cell from a square ($b = 1$) with a lateral dimension a . Minimizing the free energy with respect to a yields the lateral dimension a as a function of b . We can therefore calculate the free energy (per unit area) as a function of film thickness for each number of cylinder layers.¹³ In a good approximation, the energy minima provide the stable film thickness of the terraces together with the lateral cylinder spacing for this thickness. For a single layer of cylinders which is modeled by a rectangular unit cell of stretching ratio b ($b = h_1/a_1$, see Figure 2b), we find the lateral spacing

$$a_1 = \left(\frac{5}{6}\right)^{1/3} \left(\frac{1+b}{b+b^3}\right)^{1/3} a_0 \quad (1)$$

For a square unit cell (i.e., $b = 1$) we find $a_1 = 0.94a_0$. However, the minimum free energy is obtained for a slightly stretched rectangular unit cell with a lateral spacing $a_1 = 0.97a_0$. For thicker films, this value approaches the bulk value.

The result of the calculations is compared with the experimental observations (Figure 2a, lower plot). Both data sets are in excellent agreement, although one may question whether our system is sufficiently segregated to be treated in the framework of the SST. The results of the strong segregation approach should merely be considered as a guideline as to how the observed effects can be rationalized.

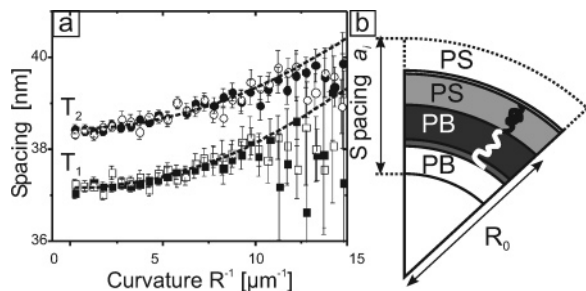


Figure 3. (a) Spacing between cylindrical microdomains as a function of the local cylinder curvature in SBS films after annealing in CHCl_3 (polymer volume fraction $\phi \approx 0.57$). The lower and the upper curves present the data in the first terrace and in the second terrace, respectively. (b) Schematic of the model used to estimate the influence of the curvature on the lateral spacing.

In essence, the flat boundary interfaces deform the hexagonal unit cell (Figure 2b). If the volume is conserved, the new geometry leads to a reduced distance between cylinders in comparison to the hexagonal unit cell.

Finally, we investigated how structural defects influence the lateral spacing. In Figure 3a the cylinder spacing is plotted versus the local lateral bending within the first and the second layer of cylinders in SBS films. In both layers, the cylinder spacing gradually increases with increasing bending curvature. The statistics are rather poor for high curvatures. On the basis of simple volume conservation arguments, the lateral spacing a_i is expected to increase quadratically with inverse bending curvature R_0 . If $a_{i,0}$ is the lateral spacing within terrace i for the case of straight cylinders, one finds

$$a_i(R_0) = a_{i,0} + \left(\frac{3}{16}\right) \frac{a_{i,0}^3}{R_0^2} \quad (2)$$

Indeed, the data are well represented by a second-order polynomial and the predicted coefficients $3/16a_{i,0}^3 = 9.6 \times 10^{-6} \mu\text{m}^3$ (for T_1 and $a_{1,0} = 39 \times 10^{-3} \mu\text{m}$) and $10.7 \times 10^{-6} \mu\text{m}^3$ (for T_2 and $a_{2,0} = 40 \times 10^{-3} \mu\text{m}$) are consistent with the values determined from the least-squares fits to the data ($9.8 \times 10^{-6} \mu\text{m}^3$ for T_1 and $8.8 \times 10^{-6} \mu\text{m}^3$ for T_2 , respectively). These results not only demonstrate the accuracy of the spacing measurement but also clearly confirm our initial statement that the presence of structural defects renders an accurate measurement of characteristic distances difficult if not impossible. For this reason only cylinders with a bending curvature of less than $5 \mu\text{m}^{-1}$ have been taken into account in the data shown in Figures 1 and 2 of this paper. We note that recently it has been shown that the distances between spherical domains measured close to a defect deviate considerably from those measured far away from any defect.¹⁸

In summary, for different annealing conditions and for model polymers with different molecular architectures, we find characteristic variations of the lateral spacing as a function of the local and overall film thickness and as a function of the lateral order (i.e., the lateral bending of a cylindrical domain). The stretching of a unit cell in thin films relative to the respective bulk structure can be qualitatively understood within the framework of the strong segregation theory. The results are most relevant both from a fundamental point of view and in view of a growing number of applications, in which control and manipulation of the characteristic distances on a nanometer scale is of utmost importance.

Acknowledgment. This project was carried out in the framework of the SFB 481 (TP B7) funded by the German Science Foundation (DFG). We thank G. J. A. Sevink for valuable comments. L.T. acknowledges financial support through the HWP program.

Supporting Information Available: Description of the determination of the characteristic spacings. This material is available free of charge via the Internet at <http://pubs.acs.org>.

References

- (1) Hamley, I. W. *Developments in Block Copolymer Science and Technology*; Wiley: Hoboken, NJ, 2004; pp 1–29.
- (2) Park, C.; Yoon, J.; Thomas, E. L. *Polymer* **2003**, *44*, 6725–6760.
- (3) Bates, F. S.; Fredrickson, G. H. *Annu. Rev. Phys. Chem.* **1990**, *41*, 525–557.
- (4) Hamley, I. W. *The physics of block copolymers*; Oxford University Press: Oxford, 1998.
- (5) Fredrickson, G. H.; Bates, F. S. *Annu. Rev. Mater. Sci.* **1996**, *26*, 501–550.
- (6) Fasolka, M. J.; Mayes, A. M. *Annu. Rev. Mater. Res.* **2001**, *31*, 323–355.
- (7) Anastasiadis, S. H.; Russell, T. P.; Satija, S. K.; Majkrzak, C. F. *Phys. Rev. Lett.* **1989**, *62*, 1852–5.
- (8) Lambooy, P.; Russell, T. P.; Kellogg, G. J.; Mayers, A. M.; Gallagher, P. D.; Satija, S. K. *Phys. Rev. Lett.* **1994**, *72*, 2899–2902.
- (9) Koneripalli, N.; Singh, N.; Levicky, R.; Bates, F. S.; Gallagher, P. D.; Satija, S. K. *Macromolecules* **1995**, *28*, 2897–2904.
- (10) Knoll, A.; Magerle, R.; Krausch, G. *J. Chem. Phys.* **2004**, *120*, 1105–1116.
- (11) Tsarkova, L.; Knoll, A.; Krausch, G.; Magerle, R. *Macromolecules* **2006**, *39*, 3608–3615.
- (12) Knoll, A.; Horvat, A.; Lyakhova, K. S.; Krausch, G.; Sevink, G. J. A.; Zvelindovsky, A. V.; Magerle, R. *Phys. Rev. Lett.* **2002**, *89*, 035501–035501.
- (13) Knoll, A. Ph.D. thesis, Universitaet Bayreuth, Germany, 2003.
- (14) Supporting Information.
- (15) Olmsted, P. D.; Milner, S. T. *Phys. Rev. Lett.* **1995**, *74*, 829–832.
- (16) Olmsted, P. D.; Milner, S. T. *Macromolecules* **1998**, *31*, 4011–4022.
- (17) Tsarkova, L. In *Nanostructured Soft Matter: Experiment, Theory, Simulation and Perspectives*; Zvelindovsky, A. V., Ed.; Springer-Verlag: 2007; pp 227–261.
- (18) Segalman, R. A.; Hexemer, A.; Hayward, R. C.; Kramer, E. J. *Macromolecules* **2003**, *36*, 3272–3288.

NL070006N